



Available online at www.sciencedirect.com



International Journal of Solids and Structures 42 (2005) 365–392

INTERNATIONAL JOURNAL OF
SOLIDS and
STRUCTURES

www.elsevier.com/locate/ijsolstr

Probabilistic energy based model for prediction of transverse cracking in cross-ply laminates

Vladimir Vinogradov ^{a,*}, Zvi Hashin ^b

^a Department of Mathematics, University of Utah, 155 S 1400 E, Salt Lake City, UT 84112, USA

^b Department of Solid Mechanics, Materials and Structures, Faculty of Engineering, Tel Aviv University, 69978 Tel Aviv, Israel

Received 12 April 2004; received in revised form 11 June 2004

Available online 18 September 2004

Abstract

In the present paper an attempt is made to describe transverse cracking of cross-ply ($[0^\circ_n/90^\circ_m]_s$) laminates subjected to an external applied load and a temperature change. For this purpose a new method is suggested which was developed on the basis of the energy balance based finite fracture criterion suggested by Hashin (1996) [Hashin, Z., 1996. J. Mech. Phys. Solids 44, 1129]. In this approach the value of the specific surface energy (the critical energy release rate) is assumed to be dependent on a random microdamage distribution in the material. Hence, it is assumed to be a random function of location. A new probabilistic technique is developed to take this randomness into consideration. It is shown that only one unknown probabilistic function is required, namely the probability density function of the specific surface energy. This is determined by fitting the external stress and the corresponding crack density to experimental data for any specific laminated system. The cracking process for any other laminate made of the same material may be predicted by the suggested method. Numerical simulation of progressive cracking process is described, which provides the probability density function for inter-crack distances as well as the crack density growth with increasing external loading. A simple probabilistic progressive cracking criterion is developed as well. The predicted crack density growth calculated for various laminates is in good agreement with published experimental results.

© 2004 Elsevier Ltd. All rights reserved.

Keywords: Cross ply laminates; Brittle fracture; Transverse cracks; Variational stress analysis; Finite fracture criterion; crack density; Probability of fracture

* Corresponding author. Tel.: +1 801 581 6898; fax: +1 801 581 4148.

E-mail addresses: vladim@math.utah.edu (V. Vinogradov), hashin@eng.tau.ac.il (Z. Hashin).

1. Introduction

The problem of damage accumulation in laminated composite materials, loaded mechanically and/or thermally, has recently received much attention due to widespread applications of laminates in the aeronautic and automotive industries. Nevertheless, the prediction of damage accumulation is still a very difficult problem due to complexity of the cracking processes.

Two most popular approaches to composite damage analysis are continuum damage mechanics and micromechanics of damage. In continuum damage mechanics all damage states are generalized into a damage tensor expressing the state of damage that can include matrix cracking, fiber breakage, interfacial debonding, or ply delamination. The composite is then treated as a continuum under states of stress and strain and the goal is to find constitutive relations between stress, strain and damage (e.g. [Talreja, 1985, 1981, 1986](#)). The approach uses no fracture mechanics or theories of crack propagation and therefore does not make any predictions about damage propagation. It only attempts to describe the relation between the mechanical properties and the level of damage, and to be useful, requires additional experimental input.

Micromechanics of damage is concerned with analysis and prediction of various types of damage. It is typically a two-step process. The first step is to use micromechanics methods to analyze the stress distribution in a composite in the presence of certain types of damage, which must be described on the basis of experimental observations (for example, matrix cracking of 90° in cross-ply laminates, or matrix cracking together with delamination, or fiber breakage of fibers in 0° layers). The stress analysis is to be carried out for stress distributions in the composite with the observed damage. This stage almost always requires approximate stress analysis due to the complexity of the problems.

After the information about the effect of observed damage on the stresses and effective material properties is estimated, the second step is to establish a failure criterion and predict the conditions under which that damage initiates and grows. It is important to note that these steps are completely independent. Any available stress analysis can be used with any failure criterion, and an appropriate approach must be developed at each of the steps.

The simplest of the laminated structures are $[0^\circ_n/90^\circ_m]_s$ laminates, also known as cross-ply laminates. This implies that the laminate consists of plies which are unidirectional fiber composites, the fiber directions in adjacent layers are orthogonal, n and m are the number of plies in each layer and s denotes symmetry. Many observations have confirmed that the first form of damage in cross-ply laminates loaded in tension is matrix cracking or microcracking in the off-axis plies. Microcracks are observed in 90° plies in which they are termed transverse cracks. Microcracks are observed during static loading, fatigue loading, thermal loading or any combination of these loadings. At the further stages of loading the transverse microcracks can promote delamination between the off-axis ply and the adjacent ply, longitudinal splitting in the 0° plies and, finally, the laminate failure. The most extensive review of the related literature published up to 1990 may be found in [Nairn and Hu \(1994\)](#).

The first systematic study of microcracking in $[0^\circ_n/90^\circ_m]_s$ laminates that includes the effect of laminate structure is the work of [Garrett and Bailey \(1977a,b\)](#); [Parvizi et al. \(1978\)](#); [Parvizi and Bailey \(1978\)](#); [Bailey et al. \(1979\)](#); [Bailey and Parvizi \(1981\)](#). Their experiments were on glass-reinforced polyester ([Garrett and Bailey, 1977a,b](#)) and glass-reinforced epoxy ([Parvizi et al., 1978](#); [Parvizi and Bailey, 1978](#); [Bailey et al., 1979](#); [Bailey and Parvizi, 1981](#)) under quasi-static loading. They varied the thickness of the 90° layer while keeping the thickness of 0° plies constant. It was shown that for thick 90° plies, the transverse microcracks originate at the edge of the specimen and propagate instantaneously through the cross-section of 90° layer. For thin plies and more ductile matrix the microcracks originate at the edge and propagate through the specimen width under the load control. Their experiments showed that the strain to initiate microcracking increases as the thickness of 90° decreases ([Parvizi et al., 1978](#)) They used careful microscopy to investigate the origins of microcrack initiation. It was found that the microcracks are generally associated with

processing flaws, voids and regions of high fiber volume fraction and initiate with debonding at the interface between the fiber and the matrix.

Continued loading generally leads to the formation of more transverse microcracks. Many investigators have carried out experiments counting the number of microcracks during quasi-static loading. Microcracks density results have been reported for different $[0^\circ_n/90^\circ_m]_s$ laminates: Boniface and Ogin (1989) Highsmith and Reifsnider (1982); Caslini et al. (1987); Wang et al. (1985); Takeda and Ogiara (1994a,b); Ogiara et al. (1997); Adolfsson and Gudmundson (1999); Yalvaç et al. (1991); Nairn et al. (1993); Liu and Nairn (1992); Nairn and Hu (1994) All the results are qualitatively similar: after formation of the first microcrack there is a rapid increase in microcrack density with increasing applied load. Eventually the rate of increasing in microcrack density slows down and it reaches a saturation level.

Due to the importance of transverse microcracking for the damaged laminate stiffness, numerous attempts have been made to compute stress distributions in the cracked laminate. The most widely used approach, found its popularity due to its simplicity, is so-called “one-dimensional analysis”. This approach was originated by Garret and Bailey in 1977 (Garrett and Bailey, 1977b) for analysis in the case of an isolated transverse crack. Manders et al. (1983) extended their results for interacting microcracks. The approach was a subject of many discussions and improvement efforts in numerous papers (see Bailey et al., 1979; Ogin et al., 1985a,b; Reifsnider, 1977; Flaggs, 1985; Fukunaga et al., 1984; Han et al., 1988; Laws and Dvorak, 1988). The method is called “one-dimensional” emphasizing the nature of the suggested assumptions: zero stresses or zero displacements in the transverse direction (z -direction in Fig. 1). The method leads to unacceptable results, such as nonzero shear stresses on the crack surfaces. So-called “two-dimensional” analysis introduced in Flaggs (1985); Fukunaga et al. (1984) considers the y -direction whose inclusion does not improve the approach and is little more than a correction for Poisson’s contraction, which is marginal from the conceptual point of view.

Some efforts have been done to avoid the deficiency of the “one-dimensional” approximation. Reifsnider (1977) introduced a shear stress transfer layer of unknown thickness and stiffness in between plies, and assumed that this layer carries only shear while the plies carry only tensile stress. A major disadvantage of this approach, called “shear-lag analysis”, is that the parameters of the shear transfer layer are unknown and must be determined by fitting to experimental results. In spite of the disadvantages of the “shear-lag” analysis and critical comments in the literature (Hashin, 1985, 1987; Nairn, 1989), it continues to grow in popularity because of its simplicity: most of its modifications can be reduced to a single differential equation

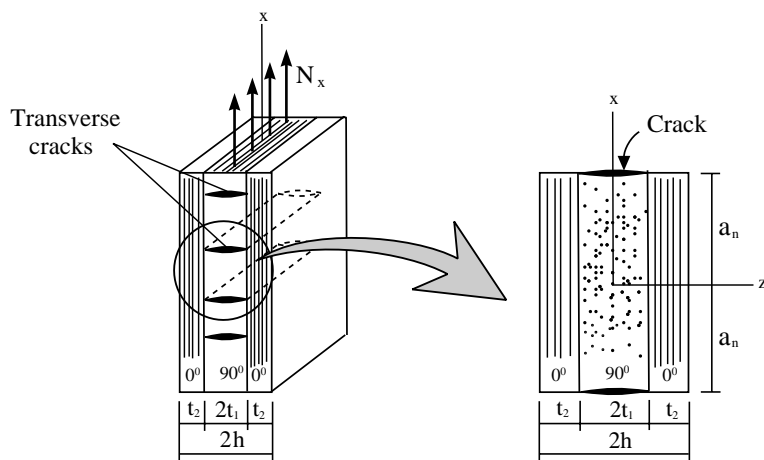


Fig. 1. Cracked cross-ply laminate loaded in tension and a typical region between two adjacent cracks.

(Nairn and Hu, 1994). Thus, the method was extended for stress distribution analysis in the presence of delamination zones around an isolated transverse crack by Dharani and Tang (1990). It is important to note, that no one-dimensional analysis can predict differences between $[0^\circ_n/90^\circ_m]_s$ and $[90^\circ_n/0^\circ_p]_s$, observed experimentally.

Finite element analysis has also been used to calculate the stress field in cracked laminates both in the presence of transverse microcracks (Wang et al., 1984) and transverse microcracks and delamination (Wang et al., 1985). The method is helpful for numerical verification of predictions of analytical approximations for stress distribution and as an “experimental measurement” of the effective stiffness of a damage material. It is limited by defining a specified stacking sequence, material properties, loading conditions and damage location, and hence, requires hundreds of calculations to describe a laminate behavior. However, finite element analysis, together with fracture mechanics, may be a unique tool capable for describing a more geometrically complex problem, such as partial microcrack, like propagating from the coupon edge in the width direction. Such solutions may be found in the literature Berthelot et al. (1996a,b, 2001).

A more accurate stress analysis approximation is a *variational approach* established by Hashin (1985, 1987, 1988). The method is based on the principle of minimum complementary energy and admissible stress fields which satisfy all boundary and equilibrium conditions. The effective stiffness of damaged laminate obtained by this stress analysis is in good agreement with the experimental results. It does not assume zero stresses in the z -direction and contains no artificial parameters, and hence, does not have the disadvantages of the “shear-lag” method. Nairn (1989) included thermal stresses into consideration and later applied Hashin’s variational mechanics analysis to the problem of transverse microcracks in $[90^\circ_n/0^\circ_p]_s$ laminate (Nairn and Hu, 1992) and delamination near the transverse crack tip (Nairn and Hu, 1991).

After a stress analysis is applied and stress fields in the presence of any damage state are found, the next step is to predict the damage development. In order to describe how microcracks will progress and which damage mode will dominate at the next moment, one has to establish a failure criterion.

Various failure criteria have been proposed in the literature. Recently, Soden et al. (1998) published an extensive review of several existing static failure theories for composite laminates, sorting them according to predicted failure modes and suggested assumption, and verifying by experimental results. A brief comparison of some failure theories for transverse cracking of laminates can be found in the surveying work by Nairn and Hu (1994).

In short, neither the numerous strength criteria (Soden et al., 1998) nor statistical theories (Fukunaga et al., 1984; Flaggs and Kural, 1982; Peters, 1984) can correctly describe various features of the phenomenon. Thus, for strength models, there is no unique critical stress/strain leading to the failure of transverse plies. Using strength theories one must consider the lamina strength as an in situ parameter depending on the stacking sequence, that discounts the method as a tool for failure prediction. Statistical strength models, based on two-parameter Weibull distribution of the 90° ply strength, fail because those parameters must also depend on laminate structure to fit experiments (Flaggs and Kural, 1982; Peters, 1984).

The failure of strength-based criteria led Parvizi et al. (1978) to propose an energy criterion. They postulated that the first microcrack forms when the energy released due to the formation of that microcrack exceeds some critical value. Since the work of Parvizi et al. (1978), the energy criterion has gained popularity and appeared in references: Parvizi and Bailey (1978); Bailey et al. (1979); Bailey and Parvizi (1981); Caslini et al. (1987); Liu and Nairn (1992); Han et al. (1988); Laws and Dvorak (1988); Nairn and Hu (1992).

Many authors used one-dimensional stress analyses to calculate the energy release rate (Garrett and Bailey, 1977b,a; Parvizi et al., 1978; Parvizi and Bailey, 1978; Caslini et al., 1987; Han et al., 1988; Laws and Dvorak, 1988). In view of disadvantages of one-dimensional stress analysis approaches, Nairn (1989) referred to Hashin’s variational method (Hashin, 1985) and found that it leads to acceptable prediction of crack initiation and accumulation. Later, Hashin (1996) developed an energy balance based brittle fracture criterion using his variational analysis. A problematic assumption about regular spaced microcracks

suggested by Nairn does not appear in Hashin's criterion. This method, called "finite fracture mechanics", was generalized and applied to various problem in Hashin (1998).

In the present paper the variational analysis is utilized to estimate the stress fields in a cracked laminate subjected to an applied load and a temperature change. The finite fracture criterion is modified to describe progressive cracking in cross-ply laminates. Within the framework of the energy balance approach, we assume randomness in the specific surface energy by relating it to a random distribution of flaws in the material. This is in contrast to the previous models, where probabilistic methods have been applied to the material strength. Taking advantage of both the energy balance based approach and the probabilistic approach, we are able to describe the growth of the crack density with applied stress in a very accurate manner. It is shown that the probability density function for the specific surface energy requires modification, being applied to different laminates. The technique for probability density function modification is developed.

2. Variational stress analysis

Let us consider a cross-ply laminate subjected to initial cool-down T from manufacturing curing temperature to the room temperature and subsequent uniform in-plane membrane tensile loading N_x in the 0° direction, Fig. 1. The average stress applied to the laminate is

$$\sigma^0 = N_x/2h,$$

where $2h$ is the laminate thickness. It is assumed that the layers can be considered as anisotropic homogeneous with effective properties of the unidirectional fiber composite. For undamaged linear elastic laminate the only existing stresses σ_{xx} in the different layers may be written

$$\begin{aligned}\sigma_{xx}^{01} &= \sigma_1 = k_1\sigma^0 + r_1T, \\ \sigma_{xx}^{02} &= \sigma_2 = k_2\sigma^0 + r_2T,\end{aligned}\tag{1}$$

where the coefficients k and r depend on laminate geometry and material properties. The subindexes 1, 2 indicate the 90° and 0° layers, respectively.

Consider now a cracked laminate, where the 90° ply has developed continuous interlaminar cracks in fiber direction and perpendicular to the plane of the laminate. The cracks are "through-the-ply" and divide the transverse ply into segments connected only by the adjacent 0° plies (Fig. 1). For the cracked laminate an admissible stress field is assumed, which satisfies equilibrium, interlaminar traction continuity and external boundary conditions, but not compatibility. The longitudinal stresses are assumed in the form (Hashin, 1985)

$$\begin{aligned}\sigma_{xx}^{a1} &= \sigma_1[1 - \phi_{1n}(x)], \\ \sigma_{xx}^{a2} &= \sigma_2[1 - \phi_{2n}(x)],\end{aligned}\tag{2}$$

where ϕ_{1n} and ϕ_{2n} are unknown functions, n stands for the n th segment between two adjacent cracks. The equilibrium equations for the plies are

$$\begin{aligned}\partial\sigma_{xx}^{ak}/\partial x + \partial\sigma_{xz}^{ak}/\partial z &= 0, \\ \partial\sigma_{xz}^{ak}/\partial x + \partial\sigma_{zz}^{ak}/\partial z &= 0,\end{aligned}\tag{3}$$

where $k = 1,2$ is the ply number. It follows that the admissible stresses within a typical region between two cracks (Fig. 1) are given by

$$\begin{aligned}\sigma_{xx}^{a1} &= \sigma_1(1 - \phi_n(x)), & \sigma_{xx}^{a2} &= \sigma_1(1 + 1/\lambda\phi_n(x)), \\ \sigma_{xz}^{a1} &= \sigma_1\phi'_n(x)z, & \sigma_{xz}^{a2} &= (\sigma_1/\lambda)\phi'_n(x)(h - z), \\ \sigma_{zz}^{a1} &= \sigma_1\phi''_n(x)(ht_1 - z^2)/2, & \sigma_{zz}^{a2} &= (\sigma_1/\lambda)\phi''_n(x)(h - z)^2/2.\end{aligned}\quad (4)$$

Here $\phi_n(x) = \phi_{1n}(x)$, $\lambda = t_2/t_1$, t_1 and t_2 are the ply thicknesses, primes denote x differentiation.

Since normal and shear stress must vanish on crack surfaces $x = \pm a_n$ the function ϕ_n must satisfy the boundary conditions

$$\phi_n(\pm a_n) = 1; \quad \phi'_n(\pm a_n) = 0. \quad (5)$$

An optimal function $\phi_n(x)$ is constructed by utilization of the principle of minimum complementary energy. Substituting the admissible stress (4) into the expression for the complementary energy

$$U_C^a = \frac{1}{2} \int_V S_{ijkl} \sigma_{ij}^a \sigma_{kl}^a \, dV,$$

where S_{ijkl} is the compliance tensor of the unidirectional fiber reinforced material, $i, j, k, l = x, y, z$. Solving the variational problem for ϕ_n , the following Euler–Lagrange equation and the boundary conditions are obtained

$$\frac{d^4 \phi_n}{d\xi^4} + p \frac{d^2 \phi_n}{d\xi^2} + q \phi_n = 0, \quad \phi_n(\pm \rho_n) = 1, \quad \phi'_n(\pm \rho_n) = 0, \quad (6)$$

where

$$\begin{aligned}\xi &= x/t_1, \quad \rho_n = a_n/t_1, \quad p = (C_{02} - C_{11})/C_{22}, \quad q = C_{00}/C_{22}, \\ C_{00} &= 1/E_T + 1/\lambda E_A, \quad C_{02} = \frac{v_T}{E_T}(\lambda + 2/3) - \frac{v_A}{3E_A}\lambda, \\ C_{22} &= (\lambda + 1)(3\lambda^2 + 12\lambda + 8)/60E_T, \quad C_{11} = (1/G_T + 1/\lambda G_A)/3.\end{aligned}\quad (7)$$

The elastic properties are: E_A the axial Young's modulus in fiber direction, v_A the associated axial Poisson's ratio, E_T the transverse Young's modulus, v_T the associated transverse Poisson's ratio, G_A the axial shear modulus and G_T the transverse shear modulus.

The characteristic equation of (6) is

$$r^4 + pr^2 + q = 0, \quad (8)$$

which produces four roots of the complex form $\pm(\alpha \pm i\beta)$ where $i = \sqrt{-1}$, or real $\pm\alpha$, $\pm\beta$, depending on values of the coefficients p and q . For widely used materials and stacking geometries the complex form of the roots is relevant. In this case the solution of the differential equation (6) provides

$$\phi_n(\xi) = A_n \cosh(\alpha\xi) \cos(\beta\xi) + B_n \sinh(\alpha\xi) \sin(\beta\xi), \quad (9)$$

where

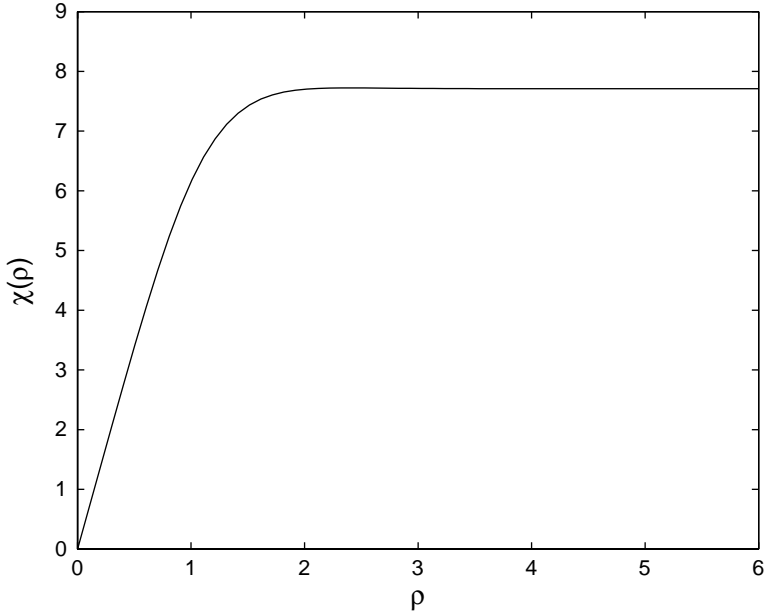
$$A_n = 2 \frac{\alpha \cosh(\alpha\rho_n) \sin(\beta\rho_n) + \beta \sinh(\alpha\rho_n) \cos(\beta\rho_n)}{\alpha \sin(2\beta\rho_n) + \beta \sinh(2\alpha\rho_n)},$$

$$B_n = 2 \frac{\beta \cosh(\alpha\rho_n) \sin(\beta\rho_n) - \alpha \sinh(\alpha\rho_n) \cos(\beta\rho_n)}{\alpha \sin(2\beta\rho_n) + \beta \sinh(2\alpha\rho_n)}.$$

This defines the admissible stress field (4).

Calculation of the complementary energy change due to transverse crack presence leads to

$$\Delta U_C^a = \sigma_1^2 t_1^2 C_{22} \sum_n \chi(\rho_n) \quad (10)$$

Fig. 2. Plot of χ function.

where the sum is over all blocks bounded by adjacent cracks and

$$\chi(\rho_n) = -\left. \frac{d^3\phi_n}{d\xi^3} \right|_{\rho_n} = 2\alpha\beta(\alpha^2 + \beta^2) \frac{\cosh(2\alpha\rho_n) - \cos(2\beta\rho_n)}{\alpha \sin(2\beta\rho_n) + \beta \sinh(2\alpha\rho_n)}. \quad (11)$$

A typical plot of function $\chi(\rho)$ for a graphite/epoxy laminate is shown in Fig. 2. It should be noted that when the cracks are far apart the function achieves its asymptotic value, which is equal to

$$\chi(\infty) = 2\alpha(\alpha^2 + \beta^2). \quad (12)$$

3. Energy based cracking criterion

Assume that the number of transverse cracks due to an external mechanical load and temperature change increases spontaneously from N_n to N_{n+1} . According to Hashin (1996), the energy release $\Delta\Gamma_n$ at n th step of the brittle cracking process may be expressed as:

$$\Delta\Gamma_n = U_C(\sigma^{n+1}) - U_C(\sigma^n), \quad (13)$$

where U_C is a complementary energy, σ^n and σ^{n+1} are the stress fields before and after formation of new cracks. The main assumption here is that these new cracks appear instantly, and the external load does not change during the process of new crack formation. Thus, both σ^n and σ^{n+1} are evaluated at the same external load. The right side of this equation may be rewritten by adding and subtracting the complementary energy of an uncracked laminate subjected to the current loads

$$\Delta\Gamma_n = [U_C(\sigma^{n+1}) - U_C(\sigma^0)] - [U_C(\sigma^n) - U_C(\sigma^0)], \quad (14)$$

where σ^0 is the stress in the undamaged material due to the same external load. The expressions in the two brackets are known on the basis of the variational approach (Hashin, 1996), yielding

$$\Delta\Gamma_n = \frac{1}{2} \int_V \Delta\sigma^{n+1} S \Delta\sigma^{n+1} dV - \frac{1}{2} \int_V \Delta\sigma^n S \Delta\sigma^n dV, \quad (15)$$

where

$$\Delta\sigma^{n+1} = \sigma^{n+1} - \sigma^0,$$

$$\Delta\sigma^n = \sigma^n - \sigma^0$$

and the stress fields include both mechanical and thermal parts.

The integrals in the right-hand side of Eq. (15) represent complementary energy difference between two states: the uncracked and cracked laminate under the same loading conditions. This complementary energy change has been approximated using variational mechanical analysis for the purpose of estimation of the stress field and given by Eq. (10). Assuming (10) is an accurate approximation of the energy change, $\Delta\Gamma$ obtains the form

$$\Delta\Gamma_n = \sigma_1^2 t_1^2 C_{22} \sum_i^{N_{n+1}} \chi(\rho_i^{n+1}) - \sigma_1^2 t_1^2 C_{22} \sum_i^{N_n} \chi(\rho_i^n), \quad (16)$$

where σ_1 is the stress in undamaged 90° ply, ρ_i^n is the nondimensional crack spacing for i th block at n th cracking step, N_n and N_{n+1} are the number of cracks before and after new crack formation, respectively, and χ is defined by (11).

Let us assume that there exists a material property γ , which defines the required energy to separate material bulk and create a unit of new free surface, such that

$$\Delta\Gamma_n = \gamma \Delta A_n \quad (17)$$

where ΔA_n is the area of newly formed cracks. The introduced parameter γ is the specific surface energy, and being defined as an energy release per unit area, it is analogous to the critical energy release rate, widely used in the fracture mechanics. However, in order to emphasize that cracks instantly occupy a finite area, we will sometimes call γ the critical energy release.

Substituting

$$\Delta A_n = A_{n+1} - A_n = t_1 (N_{n+1} - N_n)$$

we obtain

$$\gamma = \frac{\sigma_1^2 t_1^2 C_{22} \left[\sum_i^{N_{n+1}} \chi(\rho_i^{n+1}) - \sum_i^{N_n} \chi(\rho_i^n) \right]}{t_1 (N_{n+1} - N_n)}. \quad (18)$$

By averaging (18) can be written as follows:

$$\gamma = \frac{\sigma_1^2 t_1 C_{22} (N_{n+1} \bar{\chi}^{n+1} - N_n \bar{\chi}^n)}{(N_{n+1} - N_n)}. \quad (19)$$

By representing the mean $\bar{\rho}$ as a continuous variable, one can write

$$\bar{\chi}^{n+1} = \bar{\chi}^n + \frac{d\bar{\chi}^n}{d\bar{\rho}} \Delta \rho^n, \quad (20)$$

$$\Delta \bar{\rho}^n = \frac{A_{n+1}}{t_1} - \frac{A_n}{t_1} = -\frac{L}{2t_1} \frac{(N_{n+1} - N_n)}{N_{n+1} N_n}, \quad (21)$$

where the overbar denotes mean values and L is the laminate length. Substituting this into (19) it may be shown that the above equation takes the form

$$\gamma = \sigma_1^2 t_1 C_{22} \left(\bar{\chi} - \frac{d\bar{\chi}}{d\bar{\rho}} \bar{\rho} \right). \quad (22)$$

After simple transformation the right-hand side of Eq. (22) may be rewritten

$$\gamma = -\sigma_1^2 t_1 C_{22} \frac{d}{d\bar{\rho}} \left(\frac{\bar{\chi}}{\bar{\rho}} \right) \bar{\rho}^2. \quad (23)$$

Hashin (1985) has shown that the lower bound of Young's modulus of a cracked laminate is defined by

$$\frac{1}{E_x^*} = \frac{1}{E_0} + k_1^2 \frac{t_1}{h} C_{22} \frac{\bar{\chi}}{\bar{\rho}}, \quad (24)$$

where $k_1 = \sigma_1/\sigma_0$ in the case when the temperature change is absent. Using the relation for the crack area

$$A = \frac{L}{2\bar{\rho}}$$

and substituting this together with (24) into (22) one can obtain

$$\gamma = \frac{\sigma_0^2}{2} \frac{d}{dA} \left(\frac{1}{E_x^*} \right) V, \quad (25)$$

where V is the laminate volume. The latter equation is a particular uniaxial homothermal case of general fracture criterion derived in Hashin (1988)

$$\gamma = \left[\frac{1}{2} \bar{\sigma} \frac{\partial \mathbf{S}^*}{\partial A} \bar{\sigma} + \frac{\partial \boldsymbol{\alpha}^*}{\partial A} \bar{\sigma} T - \frac{1}{2} \frac{\partial c_p^*}{\partial A} \frac{T^2}{T_r} \right] V$$

where \mathbf{S}^* is the effective elastic compliance tensor, $\boldsymbol{\alpha}^*$ is the effective thermal expansion tensor, c_p^* is the effective specific heat of a composite and T_r is a reference temperature.

Regarding the statistical nature of the variable ρ , the following may be written:

$$\bar{\chi} = \int_0^\infty \chi(\rho) p(\rho) d\rho,$$

$$\bar{\rho} = \int_0^\infty \rho p(\rho) d\rho,$$

where $p(\rho)$ is a probability density function (PDF) of distances between adjacent cracks, which varies with the cracking progression. For a known $p(\rho)$ and γ , which is assumed to be a material property, Eq. (22) describes both crack propagation ($\bar{\rho}$ as a function of applied load) and cracking initiation (the least σ_1 which leads to the first crack formation). In the latter case substituting $\rho \rightarrow \infty$, Eq. (22) obtains exactly the same form as has been obtained before in Hashin (1996):

$$\gamma = \sigma_1^2 t_1 C_{22} \bar{\chi}_\infty = \sigma_1^2 t_1 C_{22} \chi(\infty). \quad (26)$$

Here the fact that for a large ρ the function $\chi(\rho)$ becomes constant and independent of ρ is taken into account (see Fig. 2), that implies

$$\bar{\chi} = \int \chi(\infty) p(\rho) d\rho = \chi(\infty) \int p(\rho) d\rho = \chi(\infty), \quad \frac{d\bar{\chi}}{d\bar{\rho}} = 0.$$

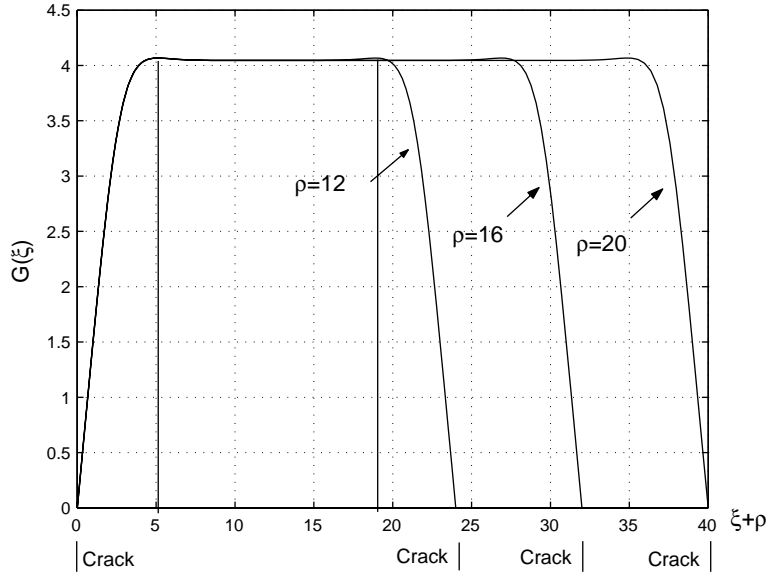


Fig. 3. Mechanical energy release as a function of the new crack location x measured from the left existing crack, for large distances between cracks.

In fact, this means that when the right-hand side of (26), which varies with laminate structure and the loading conditions, reaches the value γ which is a material property, the first crack forms. An essential feature of (22) is that its particular form (26) holds valid until high crack densities. This results in very fast initial crack density growth without additional load applying.

At the same time, any block between two existing adjacent cracks may be considered separately. Each of these blocks has the same admissible stress field and during cracking must satisfy the criterion (19), which may be rewritten for a single block as

$$\gamma = \sigma_1^2 C_{22} t_1 \left(\chi \left(\frac{\rho + \xi}{2} \right) + \chi \left(\frac{\rho - \xi}{2} \right) - \chi(\rho) \right) \quad (27)$$

where ξ denotes the coordinate of the new crack location between the two existing cracks. Equation (27) may be called a “local” criterion for crack formation, because it deals with the location of the next crack. An example of the function in the parenthesis is plotted in Fig. 3 for three large values of ρ . It can be seen that for long blocks, there is a “noninteraction zone” where the value of the energy release has approximately the same magnitude for any long block. Thus, once the right-hand side of Eq. (27) for a large ρ reached its critical value γ and cracking is initiated, a chain of fracture events occurs until sufficiently high crack density. No additional external force is required for that and (26) is valid.

4. Probabilistic concept

The criterion (27) of new crack appearance between two existing transverse cracks, relating the stresses, material property γ , the distance between the cracks and the new crack location ξ , may be written as

$$\gamma = G(\xi), \quad (28)$$

where the mechanical energy release per unit area $G(\xi)$ is determined by the right hand side of (27).

Two probabilistic notions can be introduced: “geometrical” and “physical”. The “geometrical” probability is connected to the probability of new crack formation at one of many expected locations with equal priority, in other words, at different positions ξ , where the energy release $G(\xi)$ has the same value as the critical energy release γ . This is of primary importance in predicting a crack accumulation at the stage of initial cracking, when there is no interaction between existing cracks and the energy release $G(\xi)$ has approximately the same value on a long interval (Fig. 3). This approach is supposed to provide a probability density function $p(\rho)$ to be used with criterion (22). It is interesting to note, that for a small dispersion of ρ , one can simplify Eq. (22) assuming $\bar{\chi} \approx \chi(\bar{\rho})$. Then (22) reduces to a very simple form:

$$\gamma = \sigma_1^2 t_1 C_{22} \left(\chi(\bar{\rho}) - \frac{d\chi(\bar{\rho})}{d\rho} \bar{\rho} \right). \quad (29)$$

However, some disagreements between the prediction and the experimental data are expected. First, the above approach will predict fast increase of crack density when reaching the stress of cracking initiation, up to rather high values of the crack density. Contrary to the expectations, experiments demonstrate smooth, sometime sufficiently slow dependence of crack density growth with external loading (e.g. [Nairn and Hu, 1992](#)). The question also arises as to why the conclusion, directly following from the local energy criterion, that at high crack densities, new cracks appear in the middle between two existing cracks is not supported experimentally.

These disagreements may be explained by identifying the critical energy for new surface formation as a local material property. Inhomogeneities, such as local fiber fraction, interface area between matrix and fibers, local flaw concentration in the matrix and interface, interphase fracture toughness etc. may sufficiently decrease the cracking energy at some locations: *less applied force is required to produce a crack in a cross-section which contains many flaws and weak interface*. In fact, we relate the value of γ to the local flaw concentration in a material volume element, emphasizing the sensitivity of the critical energy release rate to the local physical heterogeneity of the material. As an immediate conclusion from the arguments, we can assume that the critical energy release rate γ is a function of location. We can also deduce that the values of γ have a stochastic nature, because defect distribution throughout volume is random.

Hence, the “physical” probability is related to the critical energy release γ . An essential feature of the critical energy release γ is its sensitivity to preexisting flaws, manufacturing defects or heterogeneities in general. Therefore, γ should be considered not as a constant, rather as a stochastic function of a location with some PDF. Dealing with “through-the-ply” transverse cracks, the parameter γ may be considered as variable along the laminate direction. Thus, the criterion (28) is satisfied when at any point ξ the probabilistic “physical” γ coincides with the “mechanical” energy release $G(\xi)$

$$\gamma(\xi) = G(\xi). \quad (30)$$

Accordingly, both the “geometrical” (location of newly formed cracks) and “physical” (γ distribution) probabilities are included in the formulation and analysis. Here account must be taken of random coincidence between the appearance of any value of γ at any cross-section of the transverse ply and the energy release $G(x)$ at this location. Then the decision is made about the possibility of a new crack nucleation in that transverse plane.

Within the framework of the energy criterion described above, we can write that the energy of a new crack formation of area ΔA is equal

$$\Delta\Gamma = \int_{\Delta} \int_A \gamma(x, y, z) dy dz = \bar{\gamma}(x) \Delta A, \quad (31)$$

where $\bar{\gamma}(x)$ is the crack surface average of γ , or in other words, the average energy of unit free surface area formation at the given transverse cross-section of 90° defined by coordinate x . Accordingly, it is a random function along the laminate in the load direction x . The physical nature of the local heterogeneity is not

defined here. The only parameter describing the state of the material microdamage is the critical energy release rate and its degradation may imply local flaws and interface and/or edge defects.

5. Local toughness

Some restrictions may be imposed on the random distribution $\bar{\gamma}(x)$ in view of the material heterogeneity. As known, a transverse crack crosses the 90° ply through the matrix, surrounding fibers and linking fiber–matrix interfaces (Fig. 4). Considering a typical unidirectional fiber reinforced composite with fiber volume fraction 0.6, we can deduce that from the *geometrical* point of view, only one crack may appear between two adjacent fibers in the longitudinal direction. For a layer of thickness $t_0 = 0.155$ mm and containing homogeneously distributed fibers with the diameter 0.015 mm, the interval with only one geometrically possible crack inside may be assumed as about $0.1t_0$, that includes two fiber radii and some matrix interlayer. This parameter will be verified later by fitting experimental data.

In general, one can say that a 90° ply may be divided into small intervals of length l_r along the transverse direction, such that inside each interval only one crack may *geometrically* appear. This characteristic length

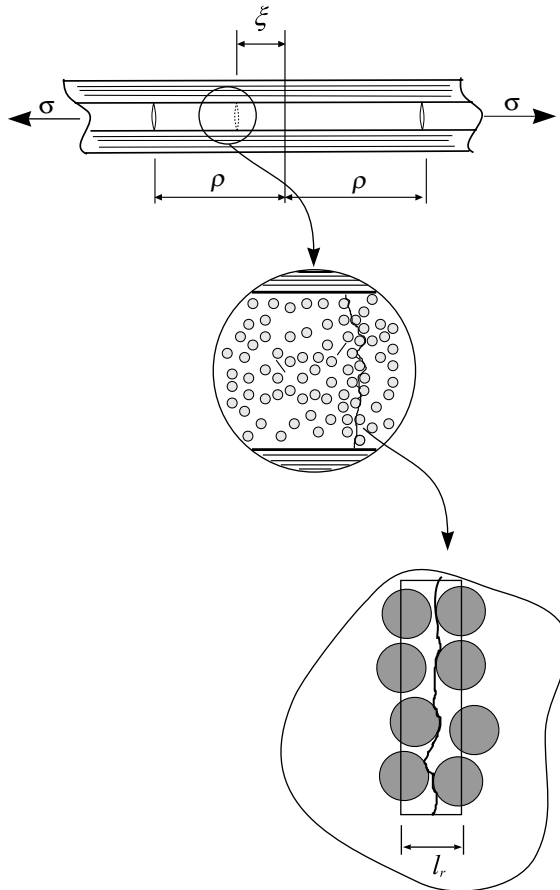


Fig. 4. Local toughness element.

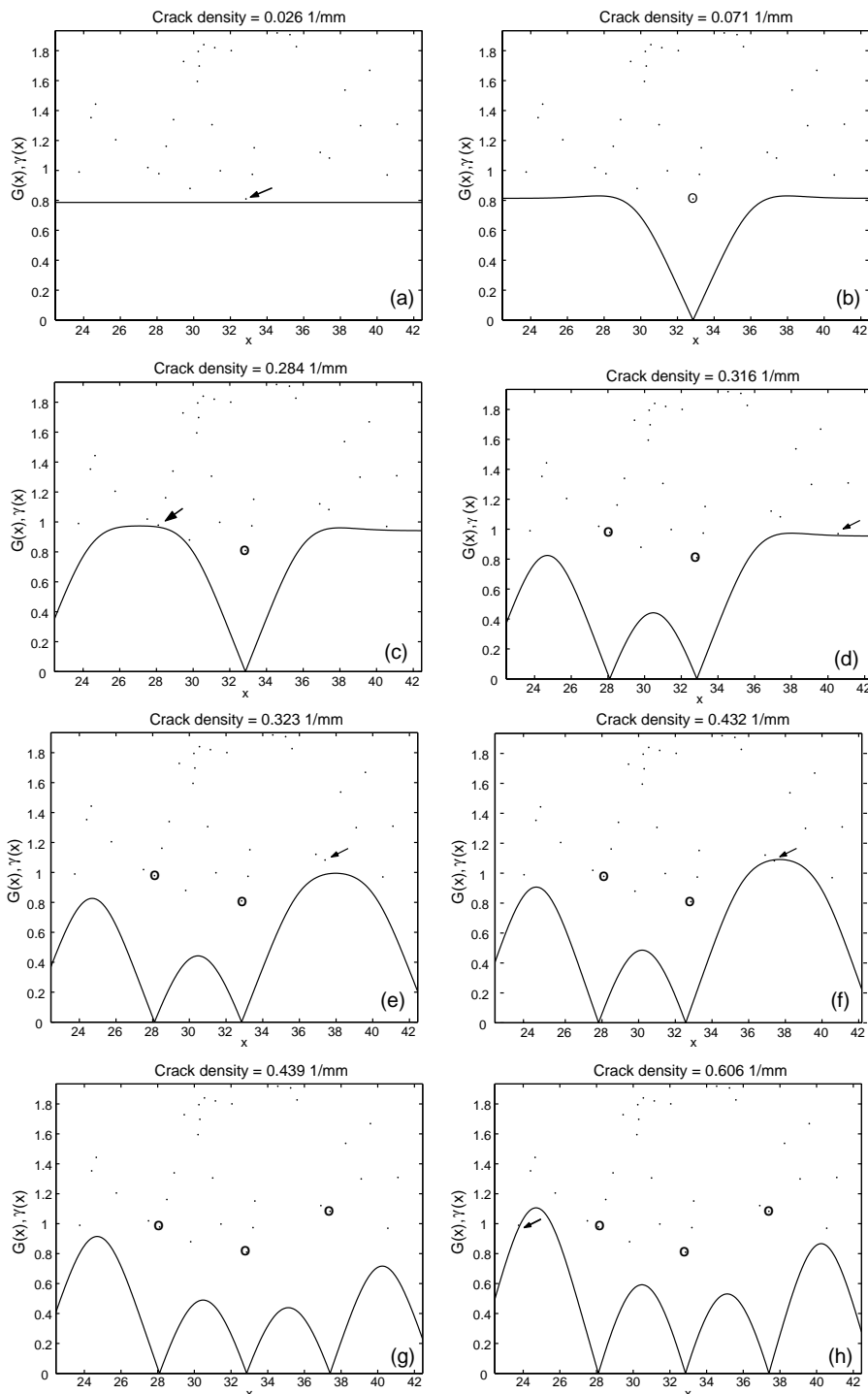


Fig. 5. The random critical energy release rate (points) and the mechanical energy release (solid line) at different steps of cracking process.

depends only on the geometrical parameters of the material, namely the fiber diameter and fiber volume fraction. If the above is correct, to each interval element l_r only one value of $\bar{\gamma}(x)$ may be assigned. It will

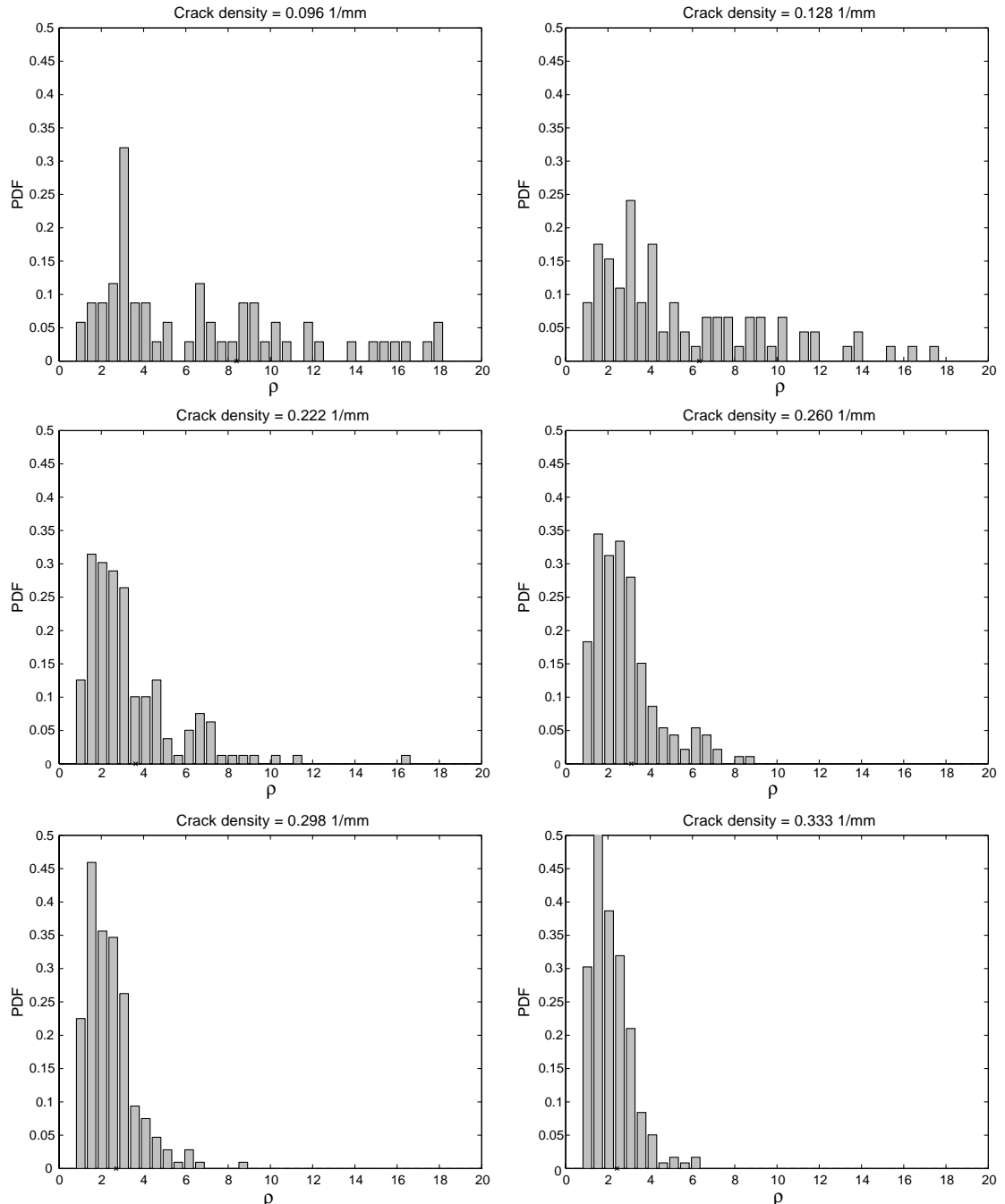


Fig. 6. An example of the probability density function transformation during progressive cracking due to increasing load.

describe the damage state inside the volume element $\Delta V = l_r h b$, where l_r is the characteristic length, h is the transverse ply thickness, and b is the laminate width. Moreover, with a high degree of confidence, the values of γ in each element l_r may be assumed to be independent from the other elements.

Imagine now a virtual experiment implying that the laminate length is cut into intervals of length l_r and measuring the $\bar{\gamma}$ values for each one. Statistical treatment of the data will provide the probability distribution function $p_r(\bar{\gamma})$ which describes a frequency of some $\bar{\gamma}$ value occurrence. Supposing that the data is representative, on the basis of this function one can model the random function $\bar{\gamma}(x)$ for any other laminate segment and build the numerical simulation of cracking process. In order to evaluate such simulation, random numbers for $\bar{\gamma}$ must be generated according to the probability density function $p_r(\bar{\gamma})$. The laminate must be divided along its longitudinal direction into elements of length l_r , in such a way that inside each element l_r only one value of random $\bar{\gamma}$ exists.

Generally, any function may be used to describe the distribution $p_r(\bar{\gamma})$. For the purpose of strength estimation, the Weibull function is usually used, which for random variable γ may be written in the following form:

$$p_r(\gamma) = \frac{\alpha}{\gamma_0} \left(\frac{\gamma - \gamma_{\min}}{\gamma_0} \right)^{\alpha-1} \exp \left[- \left(\frac{\gamma - \gamma_{\min}}{\gamma_0} \right)^\alpha \right], \quad \gamma \geq \gamma_{\min} \quad (32)$$

with the cumulative distribution function

$$P_r(\gamma) = 1 - \exp \left[- \left(\frac{\gamma - \gamma_{\min}}{\gamma_0} \right)^\alpha \right], \quad \gamma \geq \gamma_{\min}. \quad (33)$$

Here γ_{\min} is the minimal possible random variable, restricting the random variable domain for values $\gamma > \gamma_{\min}$, α and γ_0 are constant parameters of the distribution.

The random values of $\bar{\gamma}(x)$ must be compared with the mechanical energy release rate $G(x)$ in order to decide about occurrence of a cracking event. If for given stresses there is no any element located at x , such that $G(x)$ greater than $\bar{\gamma}(x)$, additional load is required to increase $G(x)$ for new crack formation. In Fig. 5 several steps of such simulation are presented. Fig. 5(a) shows a uniform function $G(x)$ for an undamaged laminate under an external stress insufficient for cracking. The function was calculated by (28) and drawn by the solid line. The points represent random values of $\bar{\gamma}(x)$. The arrows indicate the nearest value of $\bar{\gamma}(x)$, which is the next potential crack location. Additional external load increase is required for the function $G(x)$ to reach this point. After that a new crack is formed at this plane and $G(x)$ vanishes at the crack location, Fig. 5(b). The “used” values of $\bar{\gamma}(x)$ are circled for identification. Subsequent growth of the applied load leads to a new crack at a plane out of the laminate segment under consideration, that is deduced observing reduced curve of $G(x)$ at the left-hand side of Fig. 5(c). As before, the next expected crack positions are pointed out by arrows. Every next appeared crack occurs at higher stress than the previous one. It can be also noted that the crack locations are not necessarily in the middle distance between the existing cracks, rather defined by the random distribution of $\bar{\gamma}(x)$, Fig. 5(c)–(e) and (h). An example of transformation of the PDF of the distances between adjacent transverse cracks is shown in Fig. 6.

6. Probability function modification for different laminated systems

According to (31) the average value of the critical energy release rate $\bar{\gamma}$ over the crack surface must be estimated. Thus dealing with through-the-ply transverse cracks, we have to evaluate the average $\bar{\gamma}$ over the 90° ply thickness t_1 . Similarly to the random distribution of the surface energy γ along the longitudinal direction assumed before, a stochastic change of γ through the 90° ply thickness is a reasonable suggestion, because the damage state may vary though the thickness.

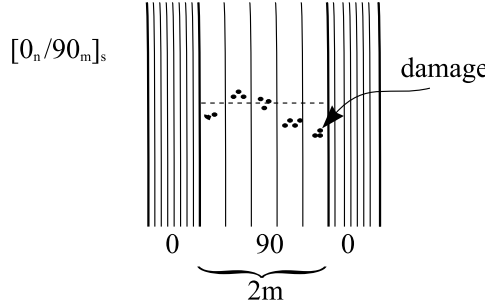


Fig. 7. Illustration of different damage states though the laminate thickness.

Now compare two laminates with stacking sequences $[0^{\circ}_{n_1}/90^{\circ}_{m_1}]_s$ and $[0^{\circ}_{n_2}/90^{\circ}_{m_2}]_s$, where the transverse plies combine $2m_1$ transverse sub-layers and $2m_2$ transverse sub-layers respectively. All the sub-layers have the same thickness t_0 and are made of the same material by the same manufacturing process. Consequently, in each sub-layer the critical energy release is described by the same probability density function $p_r(\gamma)$. However, the state of damage in the combined sub-plies at the possible new crack location x may be different due to its randomness, Fig. 7.

This yields

$$\begin{aligned}\bar{\gamma}_{2m_1} &= \frac{1}{2m_1} \sum_{i=1}^{2m_1} \gamma_i, \\ \bar{\gamma}_{2m_2} &= \frac{1}{2m_2} \sum_{i=1}^{2m_2} \gamma_i,\end{aligned}\tag{34}$$

where γ_i is the energy release rate of an element $i = 1, 2, \dots, 2m_1$ for the first laminate, in total $2m_1$ independent random variables, all with the same probability density function $p_{t_0}(\gamma)$. Similar results apply for the second stacking sequence.

As is well known from probability theory, the density function for sum z of random variables η and ζ is defined by the convolution of their probability densities:

$$h(z = \eta + \zeta) = f(\eta) * g(\zeta) \equiv \int_0^z f(\eta)g(z - \eta)d\eta.$$

Analogously, for our case we can write the probability density of the average critical energy release rate as follows:

$$p_r(\bar{\gamma}_{2m}) = \frac{1}{(2m)^{2m}} p_{t_0}\left(\frac{\gamma_1}{2m}\right) * p_{t_0}\left(\frac{\gamma_2}{2m}\right) * \dots * p_{t_0}\left(\frac{\gamma_{2m}}{2m}\right),\tag{35}$$

where all of the functions at the right-hand side are the same. The resultant function $p_r(\bar{\gamma}_{2m})$ depends on the particular form of the participating density functions. It is interesting to note that for most popular distributions like *Normal* or *Gamma* distributions, the resultant function keeps the form of the initial function, but with modified parameters.

For instant, if the *Normal* distribution function

$$p_{t_0}(\gamma) = \mathcal{N}(\gamma \mid \eta, \omega)$$

with the average η and standard deviation ω is used to fit the γ probability density function for a t_0 slice, the resultant function $p_r(\bar{\gamma}_{2m})$ obtained by (35) will be also *Normal* distribution

$$p_r(\bar{\gamma}_{2m}) = \mathcal{N}\left(\bar{\gamma} \mid \eta, \frac{\omega}{\sqrt{2m}}\right)$$

with modified standard deviation. If *Gamma* distribution function with parameters a and b is used instead

$$p_{t_0}(\gamma) = \mathcal{G}(\gamma \mid a, b) = \frac{\gamma^{a-1}}{b^a \Gamma(a)} \exp\left(-\frac{\gamma}{b}\right),$$

where $\Gamma(a)$ is the standard Gamma function, it turns to the following *Gamma* distribution where both parameters are changed

$$p_r(\bar{\gamma}_{2m}) = \mathcal{G}\left(\gamma \mid 2ma, \frac{b}{2m}\right).$$

Unfortunately, the widely used Weibull distribution does not provide such comfortable convolution as the previous examples and the resultant function must be evaluated numerically. Nevertheless, the resultant function may also be approximated with high accuracy by a Weibull function. In order to estimate the result of the convolution (35), one may take advantage of the fact that independently of the used function, the resultant convoluted function will have the same average as the initial distribution $p_{t_0}(\gamma)$ and the variance reduced proportionally to the number of participating functions:

$$\begin{aligned} \eta_{2m} &= \eta, \\ \omega_{2m}^2 &= \frac{\omega^2}{2m}. \end{aligned} \quad (36)$$

For Weibull distribution (32) the mean and the variance are defined respectively as follows:

$$\begin{aligned} \eta &= \gamma_{\min} + \gamma_0 \Gamma((1+\alpha)/\alpha), \\ \omega^2 &= \gamma_0^2 [\Gamma((2+\alpha)/\alpha) - \Gamma^2((1+\alpha)/\alpha)], \end{aligned} \quad (37)$$

where $\Gamma(x)$ is the standard Gamma function.

Comparison of the two laminated systems defined above, with help of equations (36), leads to the following relations between the corresponding averages and variances:

$$\begin{aligned} \eta_1 &= \eta_2 \\ m_1 \omega_1^2 &= m_2 \omega_2^2 \end{aligned} \quad (38)$$

where subindexes 1 and 2 denote the statistical characteristics for $[0^\circ_{n_1}/90^\circ_{m_1}]_s$ and $[0^\circ_{n_2}/90^\circ_{m_2}]_s$ stacking sequences respectively. Substitution of the mean and variance definitions for the Weibull distribution function (37) for each 90° thickness into (38), yields the following two equation system:

$$\begin{aligned} \frac{\Gamma((2+\alpha_2)/\alpha_2) - \Gamma^2((1+\alpha_2)/\alpha_2)}{\Gamma^2((1+\alpha_2)/\alpha_2)} &= \frac{m_2}{m_1} \frac{[\Gamma((2+\alpha_1)/\alpha_1) - \Gamma^2((1+\alpha_1)/\alpha_1)]}{\Gamma^2((1+\alpha_1)/\alpha_1)} \\ \gamma_{02} &= \gamma_{01} \frac{\Gamma((1+\alpha_1)/\alpha_1)}{\Gamma((1+\alpha_2)/\alpha_2)}, \end{aligned} \quad (39)$$

Table 1
Modified parameters of Weibull distribution for different laminate systems

Material	γ_{\min} (J/m ²)	$[0_n/90]_s$		$[0_n/90_2]_s$		$[0_n/90_3]_s$		$[0_n/90_4]_s$	
		α	γ_0 (J/m ²)	α	γ_0 (J/m ²)	α	γ_0 (J/m ²)	α	γ_0 (J/m ²)
Hercules 3501-6/AS4	207.9	1.0000	3.0000	1.4355	3.3040	1.7915	3.3727	2.1013	3.3872
Fiberite 934/T300	600.0	0.9362	3.1309	1.3365	3.5129	1.6649	3.6115	1.9514	3.6396
Amivid [®] K Polymer/IM6	773.5	0.8858	6.9851	1.2581	7.9728	1.5642	8.2523	1.8320	8.3449

where the parameters denoted by subindex 1 and subindex 2 are for different numbers of conjunct layers $2m_1$ and $2m_2$ respectively.

If the distribution parameters α_1 and γ_{01} of the Weibull distribution for any laminate are known (from experimental data fitting), new parameters α_2 and γ_{02} defining the probability function $p_r(\bar{\gamma})$ for another

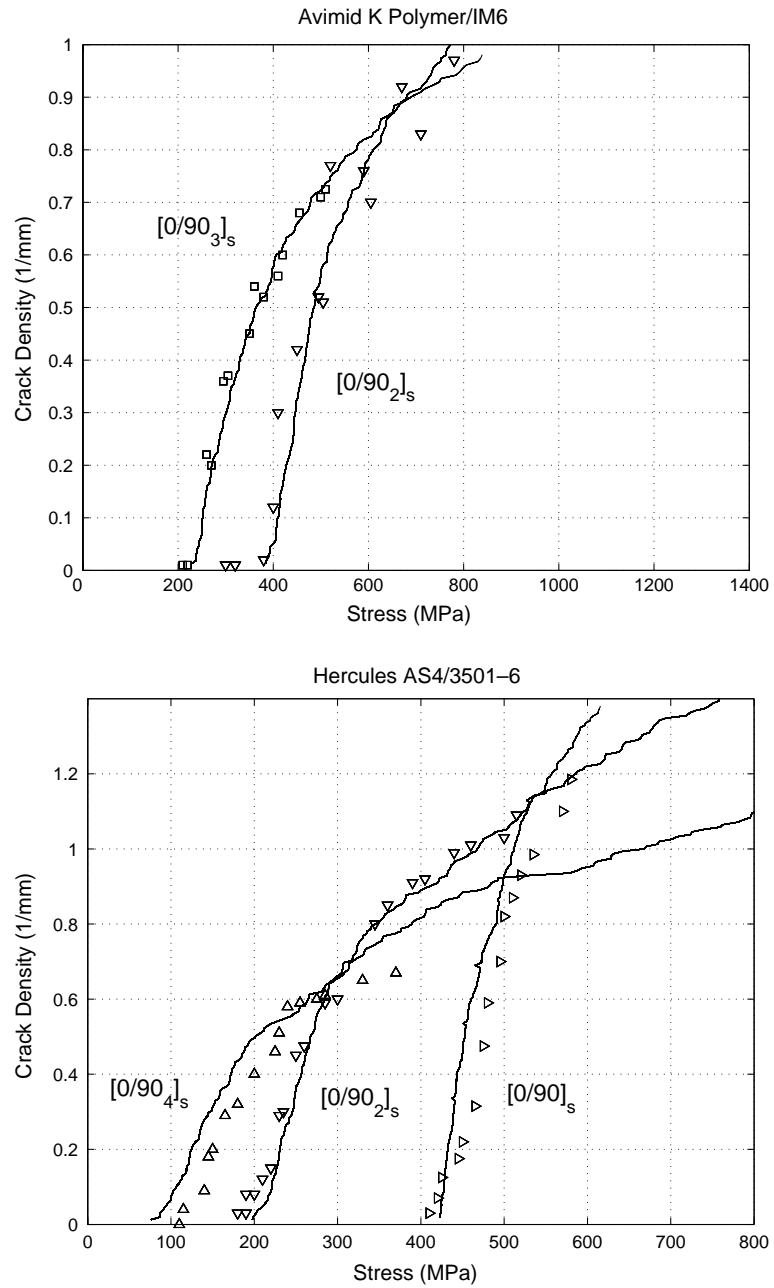


Fig. 8. Numerical simulation results.

laminate may be determined in terms of the initial parameters by solving the system (39). The first equation in (39) uniquely determines the power α_2 and being substituted to the second equation, derived from the equivalence of the means, provides the reference parameter γ_{02} . It is interesting to note here that the thicker the 90° ply and larger number of sub-layers are used for calculating the average γ , the closer the resultant function will approach the normal distribution, which is the essential feature of the convolution (35).

In order to test the model, the results of the numerical simulation proposed in Section 5 were compared with experimental data published in Liu and Nairn (1992). For each material one stacking sequence was chosen. In all the examples the random points of possible crack location were uniformly distributed along the laminates. The distance between the points l_r was varied, in order to make the convolution lead to the correct results for the crack density growth. At each point a random value of γ was generated in accordance with the Weibull distribution. The corresponding distribution parameters were estimated to fit the experimental relations between crack density and applied stress. The parameters of the Weibull distribution for the other laminate systems were calculated with the help of Eqs. (39). In all the examples the calculated reference length is about $l_r = 0.1t_0$, as it was suggested in Section 5. The results are summarized in Table 1.

Some examples of the numerical simulation results with the fitted and calculated parameters of distribution are shown in Fig. 8. It has to be noted that the deviation of the curves calculated with help of the convolution principle is in good agreement with the experimental data.

7. Probabilistic criterion of cracking

Finding the minimal strength distribution associated with unspecified flaw field in a volume element is the basic goal of the probabilistic fracture mechanics. Therefore, it is natural to use the methods of the probability theory for our purpose. We start with a simple probability treatment. Let $P(L)$ be the probability of occurrence of at least one point x^* inside a laminate segment of length L , such that the critical energy release rate at this point is equal or less than the local mechanical energy release rate at current stresses, which corresponds to the failure event in the segments

$$P(L) = P(\exists x^* \in L : \gamma(x^*) \leq G(x^*)). \quad (40)$$

The probability of the opposite event, i.e. nonoccurrence of a critical flaw inside L will be defined as $\bar{P}(L)$

$$\bar{P}(L) = \bar{P}(\nexists x^* \in L : \gamma(x^*) \leq G(x^*)) \quad (41)$$

in such a way that

$$P(L) = 1 - \bar{P}(L). \quad (42)$$

Nonoccurrence of a failure event inside L means that the critical energy release rate $\gamma(x)$ is greater than the mechanical energy release $G(x)$ at all points inside L

$$\bar{P}(L) = \bar{P}(\nexists x^* \in L : \gamma(x^*) \leq G(x^*)) = \bar{P}(\gamma(x) > G(x) \ \forall x \in L). \quad (43)$$

Let us divide the segment L into k intervals of small length Δx . Under the assumption that the probabilities of failure nonoccurrence at the intervals Δx are independent, we can rewrite the previous as:

$$\bar{P}(L) = \prod_{i=1}^k \bar{P}(\Delta x) \quad (44)$$

where the product is over all elements Δx forming L . If the probability of critical flaw occurrence is the same for all intervals Δx forming L , which corresponds to the homogeneous stress field $G(x) = G = \text{const.}$ (as observed in a undamaged laminate), the product can be replaced by a power function:

$$\bar{P}(L) = \bar{P}(\Delta x)^k = \bar{P}(\Delta x)^{L/\Delta x}. \quad (45)$$

This yields the probability of cracking inside element Δx

$$P(\Delta x) = 1 - \bar{P}(\Delta x) = 1 - \bar{P}(L)^{\Delta x/L} = 1 - (1 - P(L))^{\Delta x/L}. \quad (46)$$

Now, let us consider the segment l_r , for which the probability function of the critical flaw occurrence $P_r \equiv P(l_r)$ is known, and divide it into intervals of length Δx . An analogous treatment will lead to the following expression:

$$P(\Delta x) = 1 - (1 - P_r)^{\Delta x/l_r}. \quad (47)$$

Comparing (46) to (47) we can obtain the probability of failure event inside the interval L in terms of known probability of failure inside l_r

$$P(L) = 1 - (1 - P_r)^{L/l_r}. \quad (48)$$

If the function $G(x)$ is nonuniform along segment L , the probability of failure occurrence varies with the value of function $G(x)$. In this case we can divide L into such infinitesimal Δx , that the function $G(x)$ may be assumed constant along the element. Hence,

$$P(L) = 1 - \prod_{i=1}^k (1 - P(\Delta x_i)). \quad (49)$$

For any Δx located at x_i Eq. (47) may be rewritten as follows:

$$P(\Delta x) = 1 - (1 - P_r(x_i))^{\Delta x/l_r}, \quad (50)$$

where

$$P_r(x_i) \equiv P(\exists x^* \in l_r : \gamma(x^*) \leq G(x_i))$$

is the probability of cracking inside the reference length l_r under the external loads producing the same mechanical energy release as at the location x_i . Thus, substituting (50) into (49) one can obtain

$$P(L) = 1 - \prod_{i=1}^k (1 - P_r(x_i))^{\Delta x/l_r}. \quad (51)$$

The product in the right-hand side of Eq. (51) may be replaced by summation

$$P(L) = 1 - \exp \left(\sum_{i=1}^k \ln(1 - P_r(x_i))^{\Delta x/l_r} \right) \quad (52)$$

and taking the limit $\Delta x \rightarrow 0$ the above equation is rewritten as following:

$$P(L) = 1 - \exp \left(- \int_0^L \ln \left(\frac{1}{1 - P_r(x)} \right) \frac{dx}{l_r} \right). \quad (53)$$

This defines the probability of failure event occurrence under certain loading conditions inside a laminate segment of length L .

Let us consider a laminate segment of length l between two neighboring transverse cracks and assume that the probability function P_r is known. In Fig. 9 the energy release rate as a function of possible crack location is schematically shown together with corresponding probability $P_r(x)$ which assumes an existence of minimal value γ_{\min} . The lowest curve corresponds to the external load at the moment when the energy release function $G(x)$ reaches γ_{\min} at its highest point (σ_1 in Fig. 9). In principle, new crack formation becomes possible at this point, but the probability of this event is negligible, because an occurrence of specific value γ_{\min} at specific location is almost impossible. In order to increase the probability of cracking and

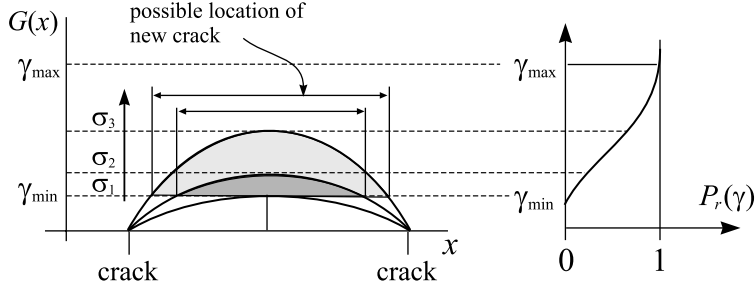


Fig. 9. Possible locations of new crack appearance for different stress levels ($\sigma_1 < \sigma_2 < \sigma_3$).

make it reach a reasonable value, the external load must be increased. This increases the values of function $G(x)$ and introduces them into the range of existing values of the critical energy release rate: $P_r > 0$. The higher $G(x)$ values above γ_{\min} the greater the probability of failure.

At the same time, the range of possible locations of a new crack appearance expands, approaches the block edges and moves away from the block middle (compare possible location ranges for σ_1 , σ_2 and σ_3 in Fig. 9). The deeper $G(x)$ gets into the range of existing γ , the wider the interval becomes where a new crack may appear inside. Thus we take into account that the probability of a new crack formation is not necessarily in the middle distance between two adjacent cracks.

The described phenomenon has a profound effect on the relation between the stress and crack density especially during cracking initiation. A shorter block will reach some cracking probability at higher stresses than a longer one, in contrast to the energy criterion for deterministic surface energy γ which provides the same cracking stress for all blocks with noninteractive zone between cracks. Hence, slower increase in crack density with external load applying is observed compared to that obtained for deterministic γ .

8. Probabilistic criterion of progressive cracking

Consider a cracked laminate of length L_0 subjected to external tensile stress σ . It may be represented as a sequence of blocks of lengths $l_i, i = 1, 2, \dots, n$. Thus Eq. (53) obtains the form

$$P(L_0) = 1 - \exp \left(- \int_{\sum_i l_i} \ln \frac{1}{1 - P_r(x)} \frac{dx}{l_r} \right) = 1 - \exp \left(- \sum_i \int_{l_i} \ln \frac{1}{1 - P_r(x)} \frac{dx}{l_r} \right). \quad (54)$$

For simplicity the above equation may be rewritten by averaging

$$P(L_0) = 1 - \exp(-n\bar{I}) \quad (55)$$

where n is a number of blocks forming the laminate of length L_0 and \bar{I} is an average integral defined as following:

$$\bar{I} = \int_0^{L_0} p(l) dl \int_0^l \ln \frac{1}{1 - P_r(x)} \frac{dx}{l_r}. \quad (56)$$

Here $p(l)$ is a PDF of block lengths, defined in terms of length l frequency

$$p(l) dl = \frac{n(l)}{n}$$

where $n(l)$ is a number of blocks with length inside dl neighborhood around l . The variable of integration in (56) is constrained by the laminate length L_0 .

However, the above equation, as well as (53), is not a probability of cracking, but of *random coincidence* between $\gamma(x)$ and $G(x)$. It does not imply any known data about the distribution $\gamma(x)$ along the laminate. It is like a previously unloaded laminate containing *artificial* transverse microcracks and subjected to external stresses. A real laminate has a *cracking history* providing us with additional information about the $\gamma(x)$ distribution. Taking into account that the laminate experiences cracking events from its virgin state until the current crack density, one can say that some flaws have already turned into cracks and small values of γ have already been “used” during the previous cracking and must be excluded from consideration at the current cracking stage. Moreover, if the laminate has produced a new crack due to the load σ_j at some point, proves that the rest of the laminate, except this point, has survived at this stress. This proves that there are no loaded points along the laminate with toughness less than $G(x)$ being generated at stresses σ_j .

This additional information about cracking prehistory can be taken into account by considering the constrained probability of the laminate cracking in the form

$$P_{\text{cr}} = \frac{P(\sigma_j) - P(\sigma_{j-1})}{1 - P(\sigma_{j-1})} \quad (57)$$

where $P(\sigma_{j-1})$ is the probability of random coincidence at the known previous closest state of loading without new crack formation. Such a state is the moment just before the previous crack has been formed. Then, substituting Eq. (55) into (57) one can obtain

$$P_{\text{cr}} = 1 - \exp(-n_j \bar{I}_j + n_{j-1} \bar{I}_{j-1}). \quad (58)$$

During transition from the state $j-1$ to j two events occur: (i) a new crack is formed at stresses σ_{j-1} , the values of function $G(x)$ reduce stepwise inside a cracked block, which leads to the decrease of the overall probability of cracking also; (ii) additional stress increase leads to the energy release $G(x)$ increasing along the whole laminate together with the probability of new cracking. In total, these alternating changes have minimal effect on the average integral \bar{I} , which may be represented as

$$\bar{I}_j \cong \bar{I}_{j-1} + \frac{d\bar{I}_{j-1}}{dc} \Delta c \quad (59)$$

where c is the crack density. Substituting (59) together with $n_{j-1} = n_j - 1$ into (58), the following form is obtained:

$$P_{\text{cr}} = 1 - \exp\left(-\bar{I} - n \frac{d\bar{I}}{dc} \Delta c\right). \quad (60)$$

Note, that the multiplication of a small increment of the crack density $\Delta c = 1/L_0$ by a large number of blocks $n = cL_0$ produces the finite value of the crack density c . Hence, Eq. (60) reduces to the following simple equation:

$$P_{\text{cr}} = 1 - \exp\left(-\bar{I} - \frac{d\bar{I}}{dc} c\right) = 1 - \exp\left(-\frac{d}{dc}(c\bar{I})\right)$$

or the same in terms of nondimensional average block length $\bar{\rho}$

$$P_{\text{cr}} = 1 - \exp\left(-\frac{d}{d\bar{\rho}}\left(\frac{\bar{I}}{\bar{\rho}}\right)\right).$$

The overall cracking probability P_{cr} is now assumed to be constant during the cracking process, which yields the simple differential equation

$$\frac{d}{dc}(\bar{I}c) = \ln(1 - P_{\text{cr}})^{-1}$$

with solution in the form

$$\bar{I} = \ln(1 - P_{\text{cr}})^{-1}(1 + B/c)$$

where B is a constant, which vanishes due to the initial condition at $c = 0$. Eq. (58) reduces to the simple equation

$$P_{\text{cr}} = 1 - \exp(-\bar{I}), \quad (61)$$

which is the exponential probability distribution function. The immediate conclusion from (61) is that the expected value of \bar{I} at the moment of the new crack formation corresponds to the quantile $P_{\text{cr}} = 1 - \exp(-1)$, which results in the equality:

$$\bar{I} \equiv \int_0^{L_0} p(l) dl \int_0^l \ln \frac{1}{1 - P_r(x)} \frac{dx}{l_r} = 1. \quad (62)$$

Further treatment of Eq. (62) requires an exact expression of block length distribution $p(l)$ for each step of the cracking process, or additional simplifying assumption. Such simplification becomes possible due to some observations made during numerous executions of the stochastic simulation described above. The definition of \bar{I} given in (56) implies integration over the block lengths containing points with $G(x) > \gamma_{\min}$. If this length range is narrow enough, the integral \bar{I} may be replaced by its value at a representative length l^* , which is identified with the length of the current cracking block.

$$\bar{I} = \int_0^{L_0} p(l) dl \int_0^l \ln \frac{1}{1 - P_r(x)} \frac{dx}{l_r} \cong I(l^*) = \int_0^{l^*} \ln \frac{1}{1 - P_r(x)} \frac{dx}{l_r}. \quad (63)$$

It has been observed that independent of the laminate stacking sequence or the material used, there exists a stable relation between the current cracking block length and the average length of the existing blocks. For a dominant range of the applied stresses, the ratio of the cracking block length to the average length is about 1.5 (Fig. 10)

$$l^* \approx 1.5\bar{l}. \quad (64)$$

In this case we can rewrite Eq. (62)

$$\int_0^{1.5\bar{l}} \ln \frac{1}{1 - P_r(x)} \frac{dx}{l_r} \approx 1. \quad (65)$$

Thus, for a given stress one can estimate the average between crack distance \bar{l} and corresponding average crack density $1/\bar{l}$ by satisfying (65), or solving the inverse problem of finding the required stress to form the given average crack density.

In the case when the probability distribution of the critical energy release rate P_r is described by the Weibull distribution function (33), the criterion (65) reduces to the following simple form:

$$\int_0^{1.5\bar{l}} \left(\frac{G(x) - \gamma_{\min}}{\gamma_{0m}} \right)^{\alpha_m} \frac{dx}{l_r} \approx 1, \quad G(x) \geq \gamma_{\min}. \quad (66)$$

This can be rewritten in terms of nondimensional variables as following:

$$\int_{-1.5\rho}^{1.5\rho} \left(\frac{G(\xi) - \gamma_{\min}}{\gamma_{0m}} \right)^{\alpha_m} \frac{t_1}{l_r} d\xi \approx 1, \quad G(\xi) \geq \gamma_{\min} \quad (67)$$

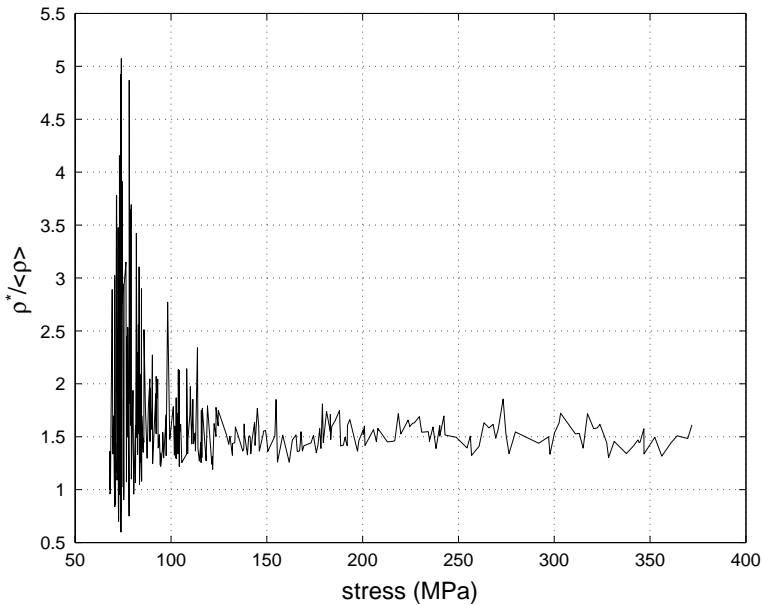


Fig. 10. Typical ratio of the cracking block length to the average length.

Table 2

The thermomechanical properties, lamina thickness and effective stress-free temperature (taken from Nairn and Hu, 1992)

Property	Amivid® K Polymer/IM6	Hercules 3501-6/AS4	Fiberite 934/T300
E_A (MPa)	134,000	130,000	128,000
E_T (MPa)	9800	9700	7200
G_A (MPa)	5500	5000	4000
G_T (MPa)	3600	3600	2400
v_A	0.3	0.3	0.3
α_A (ppm/°C)	−0.09	−0.09	−0.09
α_T (ppm/°C)	28.8	28.8	28.8
T (°C)	−225	−125	−125

where $G(\xi)$ is defined by the right-hand side of the local criterion (27)

$$G(\xi) = (k_1 \sigma^0 + r_1 T)^2 C_{22} t_1 \left(\chi \left(\frac{1.5 \bar{\rho} + \xi}{2} \right) + \chi \left(\frac{1.5 \bar{\rho} - \xi}{2} \right) - \chi(1.5 \bar{\rho}) \right). \quad (68)$$

Eq. (67) may be solved numerically for any applied stress and temperature.

The reference length l_r appearing in the current section may be chosen arbitrarily with corresponding modification of the reference parameter γ_{0m} . One can identify the length l_r with the characteristic length introduced in Section 4. For all the examples the reference length $l_r = 0.1 t_0 = 0.015$ mm leads to the best convolution results, as is concluded in Section 6. Consequently, the parameters of the distribution functions γ_{0m} and α_m correspond to P_r , and must be modified for different 90° ply thicknesses, as described above and presented in Table 1 for tested laminate systems. Other used material parameters are accumulated in Table 2.

In Figs. 11 and 12 the external applied stress versus the corresponding crack density calculated by (66) is presented for different materials and stacking sequences. The experimental data shown is taken from Nairn

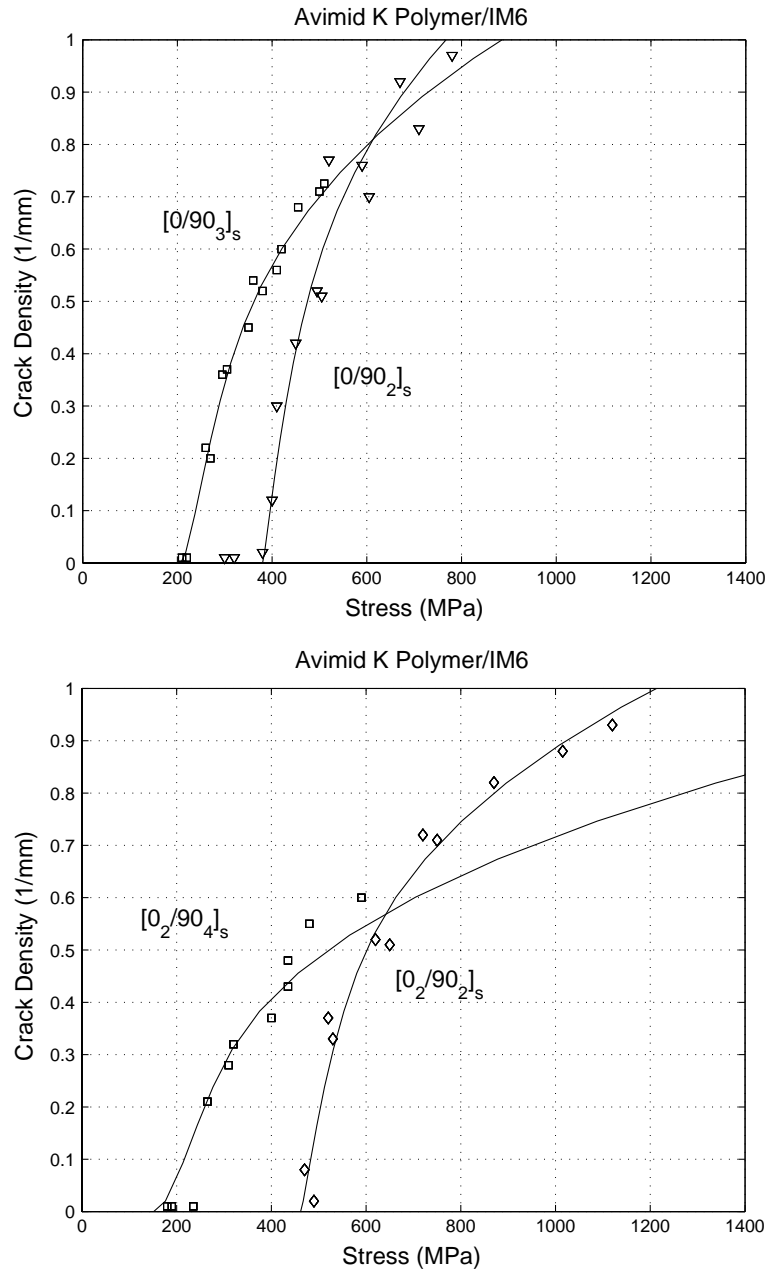


Fig. 11. Crack density vs. external applied stress.

and Hu (1992). Good agreement between the model prediction and the experiments is obtained. For some laminates (Hercules 3501-6/AS4 $[0/90]_4s$ and Fiberite 934/T300 $[0/90]_s$) a small left or right shift must be produced to fit the experiments. It may be explained by a slight mismatch in guessed thermal residual stresses through the curing temperature T , which may vary from sample to sample, due to various random disturbances during the laminate fabrication process (Fig. 12).

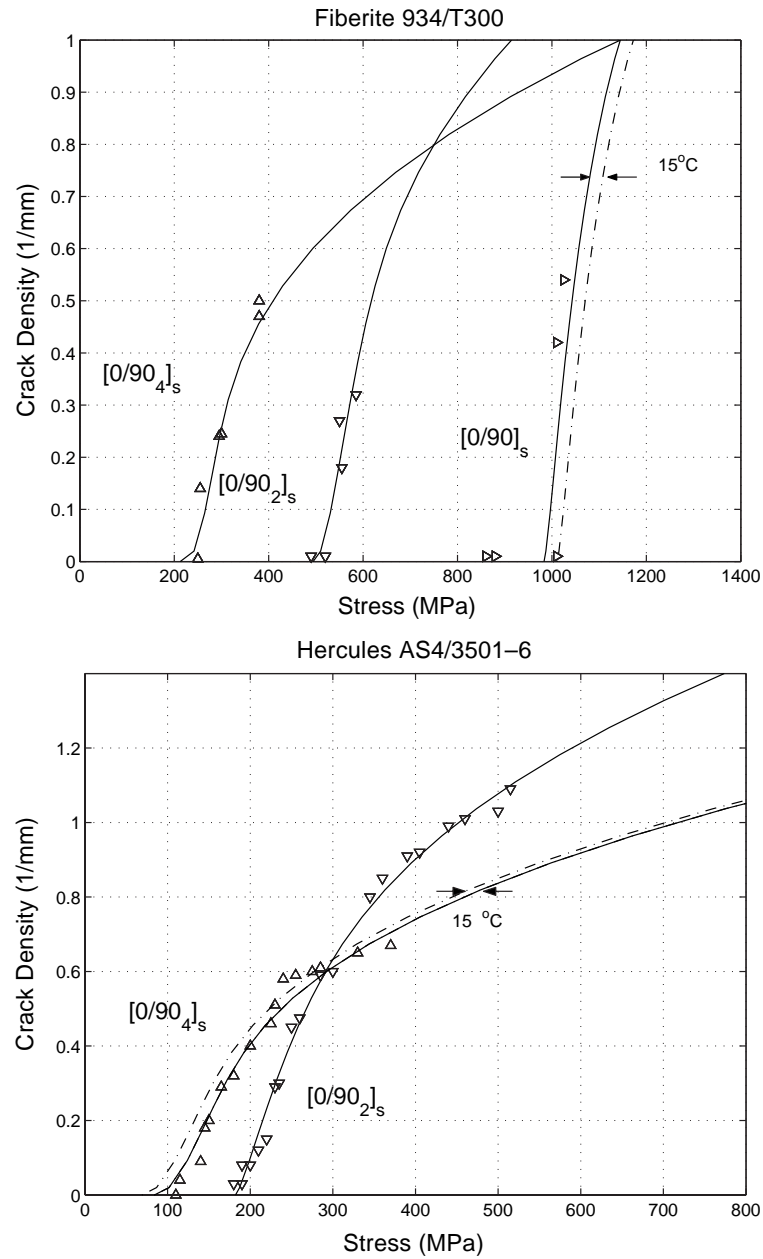


Fig. 12. Crack density vs. external applied stress.

9. Conclusion

A new method for prediction of the transverse crack accumulation due to the external mechanical and thermal load has been developed through the combination of the variation stress analysis, the finite fracture criterion and the probabilistic approach. Stochastic properties are assumed for the specific surface energy,

noticing that the energy, required for a new crack to appear, is related to a random microflaw distribution in the material.

A numerical model of the cracking process has been established, when the values of the specific surface energy, randomly distributed along the laminate, are compared to the mechanical energy release, calculated with help of the variational stress analysis and the local finite fracture criterion. The simulations provide the growth of the crack density as a function of the applied load as well as the probability density function of the inter-crack distances. The notion of the local toughness element has been introduced and discussed. The application of the finite fracture criterion implies modification of the PDF of the specific surface energy when different transverse ply thicknesses are considered. It has been shown that a convolution procedure is required, which leads to a system of coupled equations to be solved for new values of the PDF parameters.

A simple energy base probabilistic cracking criterion has been developed. The interval between the cracks wherein a new crack can appear is shown to depend on the applied stress. Smooth crack density growth with increasing external load during the initial cracking can be also explained from the probabilistic point of view. Good agreement between the transverse crack accumulation due to the external load, predicted by the suggested method, and the corresponding experimental data has been obtained.

References

Adolfsson, E., Gudmundson, P., 1999. Matrix crack initiation and progression in composite laminates subjected to bending and extension. *Int. J. Solids Struct.* 36, 3131–3169.

Bailey, J., Curtis, P., Parviz, A., 1979. On the transverse cracking and longitudinal splitting behavior of glass and carbon fibre reinforced epoxy cross-ply laminates and the effect of poisson and thermally generated strain. *Proc. R. Soc. London A* 366, 599–623.

Bailey, J., Parviz, A., 1981. On fiber debonding effects and the mechanism of transverse-ply failure in cross-ply laminates of glass fibre/thermoset composites. *J. Mater. Sci.* 16, 649–659.

Berthelot, J.-M., Leblond, P., Mahi, A.E., Le Corre, J.-F., 1996a. Transverse cracking of cross-ply laminates. Part 1: Analysis. *Composites* 27A, 989–1001.

Berthelot, J.-M., Mahi, A.E., Leblond, P., 1996b. Transverse cracking of cross-ply laminates. Part 2: progressive widthwise cracking. *Composites* 27A, 1003–1010.

Berthelot, J.-M., Mahi, A.E., Le Corre, J.-F., 2001. Development of transverse cracking of cross-ply laminates during fatigue tests. *Compos. Sci. Technol.* 61, 1711–1721.

Boniface, L., Ogin, S., 1989. Application of the Paris equation to the fatigue growth of transverse ply cracks. *J. Compos. Mater.* 23, 735–754.

Caslini, M., Zanotti, C., O'Brien, T., 1987. Study of matrix cracking and delamination in glass/epoxy laminates. *J. Compos. Technol. Res.* 9, 121–130.

Dharani, L., Tang, H., 1990. Micromechanics characterization of sublamine damage. *Int. J. Fract.* 46, 123–140.

Flaggs, D., 1985. Prediction of tensile matrix failure in composite laminates. *J. Compos. Mater.* 19, 29–51.

Flaggs, D., Kural, M., 1982. Experimental determination of the in situ transverse lamina strength in graphite/epoxy laminates. *J. Compos. Mater.* 16, 103–116.

Fukunaga, H., Chou, T., Peters, P., Schulte, K., 1984. Probabilistic failure strength analyses of graphite/epoxy cross-ply laminates. *J. Compos. Mater.* 18, 339–356.

Garrett, K., Bailey, J., 1977a. The effect of resin failure strain on the tensile properties of glass fibre-reinforced polyester cross-ply laminates. *J. Mater. Sci.* 12, 2189–2194.

Garrett, K., Bailey, J., 1977b. Multiple transverse fracture in 90° cross-ply laminates of a glass fibre-reinforced polyester. *J. Mater. Sci.* 12, 157–168.

Han, Y., Hahn, H., Groman, R., 1988. A simplified analysis of transverse ply cracking in cross-ply laminates. *Compos. Sci. Technol.* 31, 165–177.

Hashin, Z., 1985. Analysis of cracked laminates: a variational approach. *Mech. Mat.* 4, 121–136.

Hashin, Z., 1987. Analysis of orthogonally cracked laminates under tension. *J. Appl. Mech.* 109, 872–879.

Hashin, Z., 1988. Thermal expansion coefficients of cracked laminates. *Compos. Sci. Technol.* 31, 247–260.

Hashin, Z., 1996. Finite thermoelastic fracture criterion with application to laminate cracking analysis. *J. Mech. Phys. Solids* 44, 1129–1145.

Hashin, Z., 1998. Micromechanics of cracking in composite materials. In: Inan, E., Markov, K. (Eds.), *Continuum Models and Discrete Systems. Proceedings of the 9th International Symposium*. World Scientific Publishing, Singapore, pp. 702–709.

Highsmith, A., Reifsnider, K., 1982. Stiffness reduction mechanism in composite laminates. In: *Damage in Composite Materials*, ASTM STP 775, pp. 103–117.

Laws, N., Dvorak, G., 1988. Progressive transverse cracking in composite laminates. *J. Compos. Mater.* 22, 900–916.

Liu, S., Nairn, J., 1992. The formation and propagation of matrix microcracks in cross-ply laminates during static loading. *J. Reinforced Plast. Compos.* 11, 158–178.

Manders, P., Chou, T., Jones, F., Rock, J., 1983. Statistical analysis of multiple fracture in 0/90/0 glass fiber/epoxy resin laminates. *J. Mater. Sci.* 18, 2876–2889.

Nairn, J., 1989. The strain energy release rate of composite micro cracking: a variational approach. *J. Compos. Mater.* 23, 1106–1129.

Nairn, J., Hu, S., 1991. The initiation and growth of delamination induced by matrix microcracks in laminated composites. *Int. J. Fract.* 57, 1–24.

Nairn, J., Hu, S., 1992. The formation and effect of outer-ply microcracks in cross-ply laminates: a variational approach. *Eng. Fract. Mech.* 41, 203–221.

Nairn, J., Hu, S., 1994. Matrix microcracking. In: Talreja, R. (Ed.), *Damage Mechanics of Composite Materials*. Elsevier Science, Amsterdam, pp. 187–243.

Nairn, J., Hu, S., Bark, J., 1993. A critical evaluation of theories for predicting microcracking in composite laminates. *J. Mater. Sci.* 28, 5099–5111.

Ogihara, S., Takeda, N., Kobayashi, A., 1997. Experimental characterization of microscopic failure process under quasi-static tension in interleaved and toughness-improved CFRP cross-ply laminates. *Compos. Sci. Technol.* 57, 267–275.

Ogin, S.L., Smith, P., Beaumont, P., 1985a. A stress intensity factor approach to the fatigue growth of transverse ply cracks. *Compos. Sci. Technol.* 24, 47–59.

Ogin, S., Smith, P., Beaumont, P., 1985b. Matrix cracking and stiffness reduction during the fatigue of a (0/90)_s GFRP laminate. *Compos. Sci. Technol.* 22, 23–31.

Parviz, A., Bailey, J., 1978. On multiple transverse cracking in glass fiber epoxy cross-ply laminates. *J. Mater. Sci.* 13, 2131–2136.

Parviz, A., Garret, K., Bailey, J., 1978. Constrained cracking in glass fibre-reinforced epoxy cross-ply laminates. *J. Mater. Sci.* 13, 195–201.

Peters, P., 1984. The strength distribution of 90 plies in 0/90/0 graphite–epoxy laminates. *J. Compos. Mater.* 18, 545–556.

Reifsnider, K., 1977. Some fundamental aspects of the fatigue and fracture response of composite materials. In: 14th Annual Meeting of Society of Engineering Science, Bethlehem, USA, pp. 373–384.

Soden, P., Hinton, M., Kaddour, A., 1998. A comparison of the predictive capabilities of current failure theories for composite laminates. *Compos. Sci. Technol.* 58, 1225–1254.

Takeda, N., Ogihara, S., 1994a. In situ observation and probabilistic prediction of microscopic failure processes in CFRP cross-ply laminates. *Compos. Sci. Technol.* 52, 183–195.

Takeda, N., Ogihara, S., 1994b. Initiation and growth of delamination from the tips of transverse cracks in CFRP cross-ply laminates. *Compos. Sci. Technol.* 52, 309–318.

Talreja, R., 1981. Fatigue of composite materials: damage mechanisms and fatigue-life diagrams. *Proc. R. Soc. Lond. A* 378, 461–475.

Talreja, R., 1985. Transverse cracking and stiffness reduction in composite laminates. *J. Compos. Mater.* 19, 355–375.

Talreja, R., 1986. Stiffness properties of composite laminates with matrix cracking and interior delamination. *Eng. Fract. Mech.* 25, 751–762.

Wang, A., Chou, P., Lei, S., 1984. A stochastic model for growth of matrix cracks in composite laminates. *J. Compos. Mater.* 18, 239–254.

Wang, A., Kishore, N., Li, C., 1985. Crack development in graphite-epoxy cross-ply laminates under uniaxial tension. *Compos. Sci. Technol.* 24, 1–31.

Yalvaç, S., Yats, L., Wetters, D., 1991. Transverse ply cracking in toughened and untoughened graphite/epoxy and graphite/polycyanate crossply laminates. *J. Compos. Mater.* 25, 1653–1667.